

Hindrance-Functionalized π -Stacked Polymer Host Materials of the Cardo-Type Carbazole–Fluorene Hybrid for Solution-Processable Blue Electrophosphorescent Devices

Cheng-Rong Yin,[†] Shang-Hui Ye,[†] Jie Zhao,[‡] Min-Dong Yi,[†] Ling-Hai Xie,^{*,†} Zong-Qiong Lin,[†] Yong-Zheng Chang,[†] Feng Liu,[†] Hui Xu,[‡] Nai-En Shi,[†] Yan Qian,[†] and Wei Huang^{*,†}

[†]Key Laboratory for Organic Electronics & Information Displays (KLOEID) and Institute of Advanced Materials (IAM), Nanjing University of Posts & Telecommunications, Nanjing 210046, P. R. China

[‡]Key Laboratory of Functional Inorganic Material Chemistry & Ministry of Education, School of Chemistry and Materials, Heilongjiang University, Harbin 150080, P. R. China

S Supporting Information

INTRODUCTION

Phosphorescent organic light-emitting devices (PHOLEDs) have attracted tremendous research interests owing to the spin–orbit coupling interactions of heavy metals, resulting in the harvest of both singlet and triplet excitons to give the approaching 100% internal quantum efficiency theoretically.^{1–4} However, it is a prerequisite for high-performance PHOLEDs to blend the triplet emitters of heavy-metal complexes into host matrixes to reduce their concentration-quenching effect. Recently, considerable progresses have been achieved in small molecular host materials based blue PHOLEDs in terms of brightness, power efficiency, and durability.^{5–8} However, small-molecule based devices require complex coevaporation techniques, high vacuum, and tedious and precise control process during device fabrication, thus greatly hindering the success of product development and commercialization. In contrast, solution process methods, such as spin-coating, inkjet printing, or screen printing, show more advantages of easier fabrication process and lower cost with phosphorescent polymer light-emitting diodes (PPLEDs).⁹ In this context, the key issue is to develop the excellent polymer host materials for PPLEDs, especially for blue PPLEDs.

Similar to small molecular host materials, high triplet energy (E_T) levels are crucial for suitable polymer host materials to effectively prevent reverse energy transfer from emitters to hosts and confine triplet excitons on the triplet emitters in PPLEDs.^{10–12} In general, π -conjugated polymers usually have low E_T levels, which are not suitable as host materials for blue and green phosphorescent heavy-metal complexes,^{13,14} such as poly(2,7-fluorene)s and its derivatives which are the widely used π -conjugated polymer host materials possess low E_T of 2.15–2.3 eV.^{15,16} One effective method to increase the E_T levels is to design the nonlinear π -conjugated polymers via the method, limiting the delocalization length of carriers and excitons. However, the obtained π -conjugated polymers, such as poly(3,6-carbazole)s ($E_T = 2.53–2.6$ eV),^{17,18} poly(3,6-fluorene)s ($E_T = 2.58$ eV),¹⁹ poly(3,6-silafluorene)s ($E_T = 2.55$ eV),²⁰ and poly(*m*-phenylene) derivatives ($E_T = 2.64$ eV)²¹ still have too low E_T levels to act as efficient host materials for typical blue electrophosphorescent emitters, such as bis[(4,6-difluorophenyl)pyridinato-*N*, *C*²(picolinato)iridium(III) (FIrpic) ($E_T = 2.65$ eV). Other

π -conjugation-interrupted technique also provides a useful strategy to improve the E_T levels of polymer host materials through the introduction of sp^3 -hybridized carbon, silicon, or oxygen.²² However, there are still rare polymer host materials for blue electrophosphorescent emitters up to date.

With respect to π -conjugated polymers, π -stacked polymers as supramolecular semiconductors exhibit the unique carrier and exciton features in the applications of various polymer semiconducting devices.^{23,24} The design of π -stacked polymers opens another way to develop the polymer hosts for red-, green-, and blue-light-emitting triplet emitters. One typical and successful π -stacked polymer host material for triplet emitters is poly(*N*-vinylcarbazole) (PVK) with the relative high triplet energy state along with excellent hole-transporting ability,^{9,25–27} although the E_T value of PVK is still ambiguous in the reported literatures.^{14,28,29} Bilayer blue PPLEDs using PVK as polymer host exhibited power efficiency of 14 lm/W and luminous efficiency of 22 cd/A according to the reports by So and co-workers.³⁰ Nevertheless, the design of π -stacked polymer host materials with high triplet energy and bipolar carrier transporting ability affords one promising alternatives for the high-performance blue PPLEDs.^{31–36} In this paper, we proposed hindrance-functionalized π -stacked polymers to design high-triplet-energy polymer host materials for solution-processable blue electrophosphorescent devices. A model poly(*N*-vinyl-3-(9-phenylfluorene-9-yl)carbazole) (PVPFK) has been designed and synthesized. Bulky 9-phenylfluorenyl moieties (PFMs) with steric hindrance effect exhibits high E_T levels⁸ and good electron-transporting ability.³⁷ Furthermore, the introduction of PFMs into the carbazole units of PVK through the 3D cardo-type linkers of the sp^3 -hybridized carbon can not only block the intrachain face-to-face overlaps of carbazole groups but also improve the chain rigidity of PVK, resulting in high thermal and morphological stabilities. In addition, PVPFK has the enhanced electron-transporting ability with respect to PVK. PPLEDs using PVPFK as the host and FIrpic as the guest exhibited lower turn-on voltage,

Received: March 18, 2011

Revised: May 10, 2011

Published: May 31, 2011

higher efficiencies, and brightness than that of PVK-based counterpart.

EXPERIMENTAL SECTION

Chemicals and Materials. Carbazole, 1,2-dichloroethylene, 2,2'-azobis(isobutyronitrile) (AIBN), and other reagents were used as received from commercial sources. All the solvents were treated according to the standard procedures. 9-Phenylfluoren-9-ol (**1**) was prepared according to our previous report.³⁸

Characterization. ¹H and ¹³C NMR in DMSO-*d*₆ or CDCl₃ were recorded at 400 MHz using a Varian Mercury 400 plus spectrometer. Absorption and photoluminescence (PL) emission spectra of the materials were recorded on UV-3600 Shimadzu UV-vis-NIR spectrophotometer and a Shimadzu RF-5301PC spectrophotometer, respectively. The solution state spectra were measured in chlorobenzene solution. The film was prepared by spin-coating from chlorobenzene solution. Thermogravimetric analyses (TGA) were conducted on a Shimadzu DTG-60H thermogravimetric analyses with a heating rate 10 °C/min under a nitrogen atmosphere. The differential scanning calorimetry (DSC) analyses were performed on a Shimadzu DSC-60A Instrument 0 at a heating rate of 10 °C/min. Gel permeation chromatography (GPC) was used to obtain the molecular weight of the polymers with reference to polystyrene standards using THF as eluant. The cyclic voltammetric (CV) studies were conducted at room temperature on the CHI660E system in a typical three-electrode cell with a platinum sheet working electrode, a platinum wire counter electrode, and a silver/silver nitrate (Ag/Ag⁺) reference electrode. All electrochemical experiments were carried out under a nitrogen atmosphere at room temperature in an electrolyte solution of 0.1 M tetrabutylammonium hexafluorophosphate (Bu₄NPF₆) in dichloromethane (CH₂Cl₂) at a sweeping rate of 0.1 V/s. According to the redox onset potentials of the CV measurements, the highest occupied molecular orbital (HOMO)/lowest unoccupied molecular orbital (LUMO) of the materials were estimated based on the reference energy level of ferrocene (4.8 eV below the vacuum): HOMO/LUMO = $-(E_{\text{onset}} - 0.02 \text{ V}) - 4.8 \text{ eV}$, where the value 0.02 V is for FOC vs Ag/Ag⁺. The phosphorescence spectrum was tested with combined steady-state fluorescence and phosphorescence lifetime spectrometer (Edinburgh Instruments, Plsp 920). The time-resolved measurements (time-resolved emission spectra, TRES) were performed in CH₂Cl₂ glass at 77 K using time-correlated single photon counting (TCSPC) method with a microsecond flash lamp and the synchronization photomultiplier for signal collection and TCC900 plug-in PC card incorporating START and STOP constant fraction discriminators for data processing. The values of E_{T} levels of these compounds have been estimated from the onset peak of their respective phosphorescence spectrum.

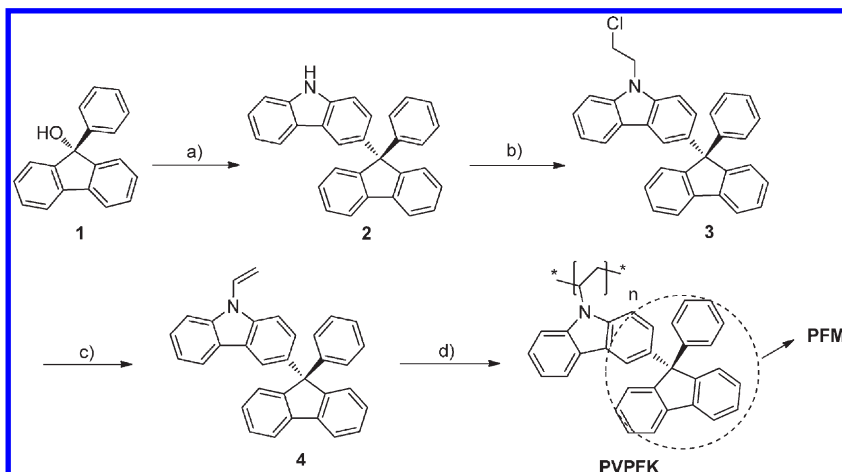
Fabrication of Phosphorescent Polymer Light-Emitting Devices. PPLEDs were fabricated in the following configuration: indium tin oxide (ITO)/poly(ethylenedioxythiophene)-poly(styrenesulfonic acid) (PEDOT:PSS, 10 nm)/host: 30% Flrpic (65 nm)/1,3,5-tris(*N*-phenylbenzimidazol-2-yl)benzene (TPBi, 40 nm)/Ca:Ag. A layer of PEDOT:PSS with thickness of 10 nm was spin-coated directly onto the ITO glass and dried at 120 °C for 20 min under vacuum to enhance the hole injection ability and to smooth the ITO substrate. The solution of the polymer was prepared under a nitrogen atmosphere and spin-coated on the PEDOT:PSS layer. The TPBi was used as an

electron-transporting/hole-blocking layer as well as excitation-confining layer. The cathode Ca:Ag alloy was subsequently deposited onto the TPBi layer. EL spectra and chromaticity coordinates were measured with a SpectraScan PR650 photometer. Current density-voltage-luminance (J - V - L) measurements were conducted simultaneously using a Keithley 4200 semiconductor parameter analyzer combined with a Newport multifunction 2835-C optical meter, with luminance being measured in the forward direction. All device characterizations were carried out under ambient laboratory air at room temperature.

Synthesis of 3-(9-Phenylfluoren-9-yl)carbazole (2). A solution of BF₃·Et₂O complex (3.73 mL, 29.37 mmol) in appropriate CH₂Cl₂ (40 mL) was added dropwise to a mixture solution of **1** (6.45 g, 24.96 mmol) and carbazole (4.16 g, 24.96 mmol) in appropriate CH₂Cl₂ (200 mL). The reaction mixture was stirred at 25 °C under nitrogen until starting material is no longer detectable by TLC. After that, ethanol (100 mL) and water (300 mL) were successively added to quench the reaction, and then organic phases were separated and the aqueous phase was extracted with dichloromethane. The combined organic phases were washed and dried over MgSO₄. After removal of the solvent, the remaining crude product was purified by silicon gel chromatography (petroleum ether/dichloromethane) to yield products. Yield: 4.98 g (49%). MS (m/z): [M^+] calcd for C₃₁H₂₁N, 407.51; found 407.20. ¹H NMR (400 MHz, DMSO-*d*₆) δ (ppm): 11.2 (s, 1H), 7.92–7.94 (d, $J = 7.3 \text{ Hz}$, 2H), 7.84–7.86 (d, $J = 8.0 \text{ Hz}$, 2H), 7.78 (s, 1H), 7.50–7.51 (d, $J = 7.4 \text{ Hz}$, 2H), 7.29–7.42 (m, 7H), 7.21–7.25 (m, 3H), 7.12–7.17 (t, 3H), 7.02–7.05 (t, 1H). ¹³C NMR (100 MHz, DMSO-*d*₆) δ (ppm): 65.5, 111.2, 111.4, 118.9, 119.1, 120.4, 120.9, 122.5, 126.0, 126.2, 126.6, 127.0, 127.9, 128.1, 128.2, 128.7, 136.0, 139.0, 139.9, 140.5, 147.0, 151.8. Anal. Calcd for C₃₁H₂₁N: C, 91.37; H, 5.19; N, 3.44. Found: C, 91.65; H, 5.23; N, 3.39.

Synthesis of 9-(2-Chloroethyl)-3-(9-phenylfluoren-9-yl)carbazole (3). **2** (15 mmol) was added to an intensity stirred mixture of 1,2-dichloroethylene (40 mL), tetrabutylammonium bromide (0.13 g, 0.4 mmol), KOH (7 g, 125 mmol), and K₂CO₃ (5.5 g, 40 mmol). The stirring was continued at 45–50 °C for 3.5–5.5 h. After cooling, the inorganic material was filtered off, and the organic solution was washed with water (2 × 25 mL). The solution was then dried over anhydrous MgSO₄ and filtered, and the solvent was evaporated to dryness. The product was purified by crystallization from ethanol. Yield: 2.68 g (38%). MS (m/z): [M^+] calcd for C₃₃H₂₄ClN, 470.00; found 470.20. ¹H NMR (400 MHz, DMSO-*d*₆) δ (ppm): 7.93–7.95 (d, $J = 7.8 \text{ Hz}$, 2H), 7.88–7.90 (d, $J = 7.7 \text{ Hz}$, 2H), 7.83 (s, 1H), 7.59–7.61 (d, $J = 8.1 \text{ Hz}$, 1H), 7.51–7.53 (d, $J = 7.6 \text{ Hz}$, 3H), 7.38–7.43 (t, 3H), 7.08–7.41 (m, 9H). ¹³C NMR (100 MHz, DMSO-*d*₆) δ (ppm): 43.4, 44.5, 65.4, 109.9, 110.0, 119.3, 119.5, 120.5, 121.0, 122.3, 122.4, 126.2, 126.3, 126.7, 127.0, 128.0, 128.1, 128.3, 128.8, 136.8, 139.3, 139.9, 140.9, 146.8, 151.7. Anal. Calcd for C₃₃H₂₄ClN: C, 84.33; H, 5.15; N, 2.98. Found: C, 84.22; H, 5.30; N, 2.91.

Synthesis of *N*-Vinyl-3-(9-phenylfluoren-9-yl)carbazole (4). A mixture of **3** (5.0 mmol), KOH (1.12 g, 20 mmol), and hydroquinone (25–30 mg, 0.22–0.27 mmol) was placed in 2-propanol (30 mL) and refluxed for 3 h. Next the alcohol was evaporated under reduced pressure, and the organic material was extracted from the reaction mixture by means of CH₂Cl₂ (3 × 20 mL). The extract was then dried over anhydrous MgSO₄ and filtered, and the solvent was evaporated to dryness. The product was purified by crystallization from methanol. Yield: 2.12 g

Scheme 1. Synthetic Route of PVKPF^a

^a Reagents and conditions: (a) carbazole, $\text{BF}_3 \cdot \text{Et}_2\text{O}$, CH_2Cl_2 ; (b) 1,2-dichloroethylene, KOH, K_2CO_3 , 45–50 °C; (c) isopropanol, KOH, hydroquinone, refluxed, 3 h; (d) AIBN, toluene, 85 °C, 2 days.

(98%). MS (m/z): $[\text{M}^+]$ calcd for $\text{C}_{33}\text{H}_{23}\text{N}$, 433.54; found 433.15. ^1H NMR (400 MHz, $\text{DMSO}-d_6$) δ (ppm): 7.93–7.95 (d, $J = 7.6$ Hz, 3H), 7.88 (s, 1H), 7.77–7.79 (d, $J = 8.3$ Hz, 1H), 7.71–7.74 (d, $J = 8.7$, 1H), 7.48–7.55 (p, 3H), 7.38–7.45 (m, 3H), 7.29–7.33 (m, 2H), 7.14–7.25 (m, 7H). ^{13}C NMR (100 MHz, $\text{DMSO}-d_6$) δ (ppm): 65.4, 79.6, 101.5, 111.3, 111.4, 119.4, 120.7, 121.2, 123.4, 123.7, 126.6, 127.1, 127.2, 128.1, 128.3, 130.1, 138.5, 139.5, 140.0, 146.6, 151.4. Anal. Calcd for $\text{C}_{33}\text{H}_{23}\text{N}$: C, 91.42; H, 5.35; N, 3.23. Found: C, 91.15; H, 5.52; N, 3.13.

Synthesis of Poly(*N*-vinyl-3-(9-phenylfluorenyl)carbazole) (PVKPF). The monomer 4 (0.433 g, 1.0 mmol) was allowed to polymerize carried out in toluene (10 mL) with 10 wt % 2,2'-azobis(isobutyronitrile) (AIBN) (0.0433 g) as initiator and refluxed under nitrogen at 85 °C for 2 days. The polymerization was stopped by pouring the reaction mixture into ethanol. The obtained polymer was purified by repeated reprecipitations followed by drying under vacuum. Yield: 0.251 g (58%). $M_n = 9047$, PDI = 1.79. ^1H NMR (400 MHz, CDCl_3) δ (ppm): 5.28–8.03 (br, ArH), 2.48 (s, CH), 2.31 (s, CH_2). ^{13}C NMR (100 MHz, CDCl_3) δ (ppm): 45.7, 57.3, 65.4, 112.1, 120.2, 123.8, 124.3, 125.3, 126.6, 127.0, 127.6, 128.2, 129.0, 129.8, 130.0, 130.5, 131.5, 140.0, 146.4, and 152.0. Anal. Calcd for $\text{C}_{33}\text{H}_{23}\text{N}$: C, 91.42; H, 5.35; N, 3.23. Found: C, 90.98; H, 5.78; N, 3.32.

RESULTS AND DISCUSSION

Synthetic routes of the monomer 4 and target PVKPF are depicted in Scheme 1 according to a reported route in the previous literature.³⁹ PFM-functionalized carbazole 2 was synthesized through Friedel–Crafts reaction using $\text{BF}_3 \cdot \text{Et}_2\text{O}$ complex as a Lewis acid catalyst in the yield of 49% according to our previous works.⁴⁰ The following nucleophilic substitution of compound 2 with dichloroethylene was carried out to give compound 3, followed by the vinylization under the condition of hydroquinone/isopropanol/KOH to give monomer 4 in the yield of 98%. Free radical polymerization of monomer 4 was conducted in toluene using AIBN as initiator in the weight ratio of 10% at 85 °C for 2 days under nitrogen to smoothly prepare

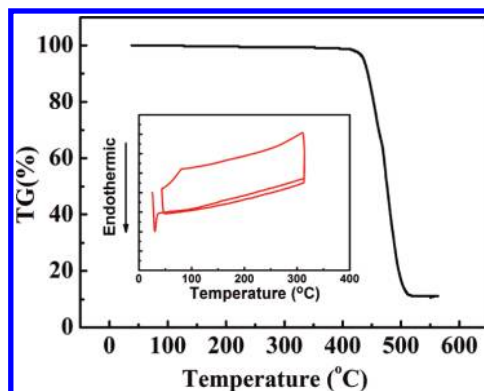


Figure 1. TGA curve of PVKPF recorded at a heating rate of 20 °C/min (decomposition temperature from the position of 5% weight loss). Inset: DSC trace of PVKPF recorded at a heating rate of 20 °C/min.

the target polymer PVKPF in a 58% yield. PVKPF is readily soluble in common organic solvents such as chloroform, tetrahydrofuran (THF), toluene, and chlorobenzene. The chemical structures of monomer and PVKPF were confirmed by ^1H NMR and ^{13}C NMR and element analysis. The number-average molecular weight (M_n) and polydispersity index (PDI) of PVKPF, as determined by GPC against a polystyrene standard in THF, were around 9×10^3 and 1.79, respectively. Thermal properties of PVKPF have been estimated by TGA and DSC. PVKPF has outstanding thermal stability with the decomposition temperature (T_d) of up to 434 °C. No glass phase transition was observed in the temperature range from 50 to 300 °C. The high thermal stability of PVKPF probably is attributed to the PFM in the 3D cardo structure, suppressing its crystallization process, which is greatly favorable for the stable polymer host materials in PPLEDs.

Photophysical Properties. Figures 2a,b compare the UV–vis absorption and PL spectra of PVKPF with the pristine PVK in diluted chlorobenzene solutions as well as in the thin film spin-coated from chlorobenzene solution. The normalized UV–vis absorption spectra of PVKPF in solution shows three strong absorption bands at 299, 336, and 349 nm, similar to that of PVK with the bands at 293, 330, and 343 nm, respectively. A

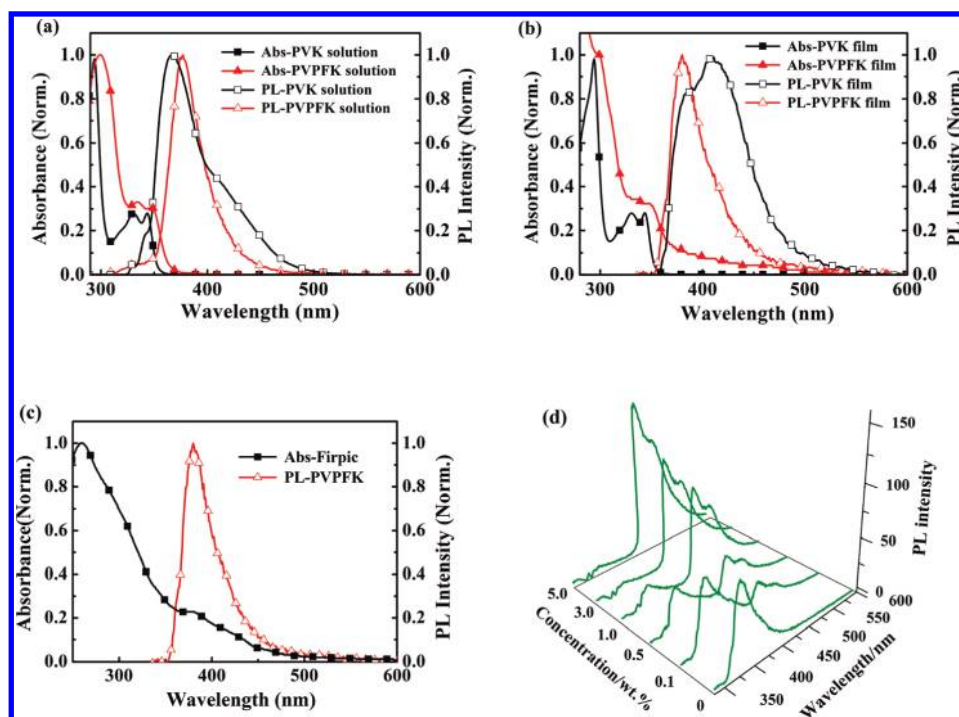


Figure 2. (a) UV–vis absorption and PL spectra of PVPFK and PVK in diluted chlorobenzene solution. (b) UV–vis absorption and PL spectra of PVPFK and PVK in the solid state. (c) Normalized UV–vis spectra of FIrpic and PL spectra of PVPFK in thin film. (d) PL spectra of thin films of PVPFK doped with various concentrations of FIrpic.

bathochromic shift of 6 nm is probably due to the hyperconjugation effect of bulky PFMs. However, the PL spectrum of PVPFK in solution is obviously different from that of PVK whose major emission peak at 367 nm and a shoulder emission peak at 400 nm. But PVPFK exhibits only one emission peak at 376 nm without any excimer emission peaks in solution; for details see Figure 2. Furthermore, PVPFK in solution have an obviously narrow emission with 9 nm red shift with respect to that of PVK. Two emission peaks of PVK in solution come from intrachain partial and full face-to-face overlaps of carbazole groups. These results suggest that no full overlapping conformation formed in PVPFK solution.⁴¹ The first emission peak exhibits a red shift of 13 nm when transferred from the solution to thin film and the intensity of emission peak at 410 nm becomes stronger, which suggest that full overlapping components increased. In contrast, the PVPFK in the thin film exhibits emission peak at 379 nm, which is slightly red-shifted (ca. 3 nm) compared with that of the solution spectrum. These results indicate that π – π stacking alignments of carbazole groups in PVPFK are effectively blocked by the bulky PFMs owing to their steric hindrance effects. The optical band gap of PVPFK was estimated to be 3.34 eV from the absorption edge of its UV–vis spectrum in thin solid film, a little smaller than that of PVK film (3.44 eV).

The phosphorescence spectra of PVPFK and PVK were also measured in CH_2Cl_2 glass at 77 K under the same conditions (Figure S1). The value of E_T level of PVPFK was estimated from the highest energy 0–0 phosphorescent emission located at 442 nm to be 2.80 eV, which was lower than that of PVK ($E_T = 2.95$ eV, 422 nm). This result is consistent with the previous reports that the introduction of fluorene into carbazole-based groups has an reduction of E_T level.⁸ However, the E_T level of 2.80 eV is high enough for PVPFK to serve as host materials for blue triplet emitters, such as FIrpic ($E_T = 2.65$ eV).

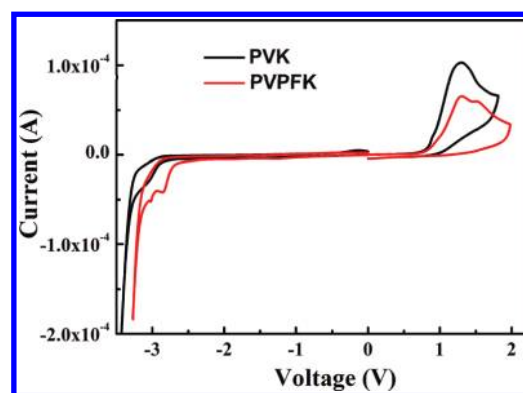


Figure 3. Cyclic voltammograms of PVPFK and PVK film on a glassy carbon electrode (0.1 MBu_4NBF_4 in acetonitrile, scan rates 20 mV/s).

Figure 2c shows the absorption spectrum of FIrpic and the PL spectrum of pure PVPFK in the solid state. There is a good overlap between the PL spectrum of PVPFK and the absorption spectrum of FIrpic, which guarantee efficient Förster energy transfer from singlet-excited state in the host (PVPFK) to metal–ligand (FIrpic) charge-transfer absorption band in the guest. In order to estimate the potential of PVPFK as a polymer host for blue phosphorescent emitters and test the efficiency of Förster energy transfer, the PL spectra of PVPFK films doped with various contents of FIrpic were investigated. Figure 2d shows the PL spectra of pure PVPFK film and the doped PVPFK films. The doping concentrations of FIrpic in PVPFK varied from 0.1%, 0.5%, 1.0%, and 3.0% to 5.0% by weight. The PL profile contains two emission peaks: one peak at 379 nm comes from the PVPFK emission, and the other peak at 473 nm comes from

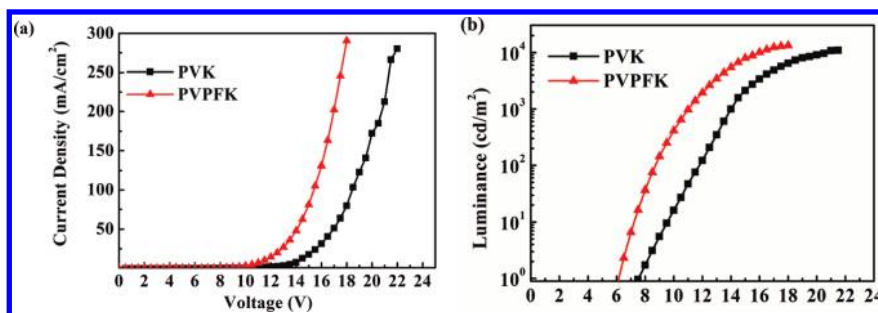


Figure 4. (a) Current density–voltage (J – V) curves of PVPFK and PVK devices. (b) Luminance–voltage (L – V) curves of PVPFK and PVK devices.

the FIrpic triplet emission. The emission intensity of the host material at 379 nm decreased with increasing doping concentration of FIrpic and was completely quenched at a doping concentration of about 5 wt %, indicating that there was an efficient Förster energy transfer from PVPFK to FIrpic.

Electrochemical Properties. CV measurement was carried out to investigate the oxidation and reduction behavior of PVPFK and estimate its HOMO and LUMO energy levels. Figure 3 displays the CV spectra of PVK and PVPFK measured under the same condition. The oxidation onset potentials were recorded at 0.80 V for PVPFK and 0.83 V for PVK versus Ag/Ag^+ , respectively. As a result, HOMO energy levels were estimated to be -5.58 eV for PVPFK and -5.61 eV for PVK according to the empirical formula $E_{\text{HOMO}} = -(E_{\text{ox}} - E_{\text{FOC}}) - 4.8$ eV, where the value of E_{FOC} for ferrocene is 0.02 V vs Ag/Ag^+ and 4.8 eV is the energy level of ferrocene below vacuum. The result indicated that the introduction of the bulky PFMs into PVK does not affect the HOMO energy level. The reduction onset potentials were measured to be -2.70 V for PVPFK and -2.88 V for PVK, from which the LUMO energy levels of PVPFK and PVK were calculated to be -2.08 and -1.90 eV, respectively, according to the empirical formula $E_{\text{LUMO}} = -(E_{\text{red}} - E_{\text{FOC}}) - 4.8$ eV, where the value of E_{FOC} for ferrocene is 0.02 V vs Ag/Ag^+ and 4.8 eV is the energy level of ferrocene below vacuum. These results suggest that PVPFK have better electron-transporting ability than that of PVK owing to the introduction of fluorene groups. In general, PVK has poor electron-transporting ability.⁴² Electron-transporting materials, such as 2-(4-biphenyl)-5-(4-*tert*-butylphenyl)-1,3,4-oxadiazole (PBD) or 1,3-bis[(4-*tert*-butylphenyl)-1,3,4-oxadiazolyl]-phenylene (OXD), were required to dope into PVK to balance the hole and electron transportation in PPLEDs. However, the risk of phase separation occurring over time could not be avoided in PVK and PBD/OXD blends based PPLEDs.^{43,44} The electrochemical characterization studies of PVPFK indicate that PVPFK could be applied as potential host material for PPLEDs directly with no need to dope with electron-transporting materials.

Electroluminescence Properties of PPLEDs. From the foregoing analysis, we know that PVPFK possesses overall better physicochemical properties and carrier transporting ability than that of pristine PVK in terms of the thermal and morphological stability, photophysical properties, and electronic structures, except for the E_{T} level (2.80 eV), making it as a potential polymer host for blue PPLEDs. To testify our assumption, blue PPLEDs were fabricated using PVPFK as blue phosphorescent host material and FIrpic as phosphorescent emitter in a simply three-layered device structure. For comparison, PVK-based devices were also fabricated by using PVK to replace PVPFK

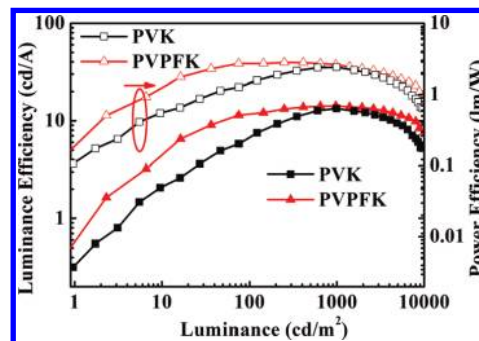


Figure 5. Luminance and power efficiency characteristic curves as a function of luminance of PVPFK and PVK devices.

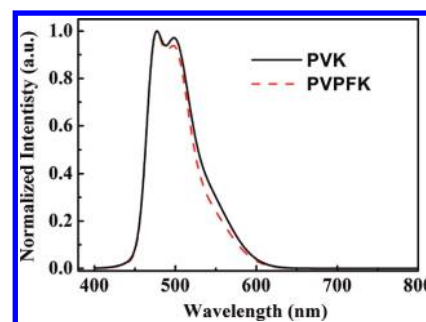


Figure 6. EL spectra of PPLEDs made from PVPFK device (dash line) and PVK device (solid line) doped with FIrpic at a mass ratio of 30 wt %.

matrix in the same device configuration. For all devices the doping concentration was controlled at 30%. The emitting layer was spin-coating from chlorobenzene solution on the PEDOT:PSS smoothed ITO glass substrate, and the electron-transporting layer of TPBi was vapor deposited under vacuum. The device architecture was ITO/PEDOT:PSS (10 nm)/host: 30% FIrpic (65 nm)/TPBi (40 nm)/Ca:Ag, where the host material was PVPFK or PVK.

Figure 4 shows the current density–voltage–luminance (J – V – L) curves of PVPFK and PVK devices. Clearly, the PVPFK device exhibited lower operation voltage and higher luminance than PVK device under the same applied voltage. For example, the turn-on voltage (recorded at a brightness of 1 cd/m^2) was 6.1 V for PVPFK device vs 7.4 V for PVK device, and the luminance of PVPFK device is higher than the PVK device in the operational voltage range. For example, the brightness of PVPFK device reached 12418 cd/m^2 at 17 V, while PVK device only exhibited 4875 cd/m^2 at the same applied voltage. Moreover, our

Table 1. Blue PPLEDs Performance Based on PVK or PVPFK Host Materials

host	V_{on} [V] ^a	L_{max} [cd/m ²]	LE_{max} [cd/A]	PE_{max} [lm/W]	LE^b [cd/A]	PE^b [lm/W]	CIE ^c [x, y]	LE^c [cd/A]	PE^c [lm/W]
PVK	7.4	10 968	13.3	2.4	6.1	1.5	0.161, 0.398	12.9	2.2
PVPFK	6.1	13 287	14.2	2.8	12.0	2.7	0.152, 0.379	14.1	2.6

^a Recorded at 1 cd/m². ^b Obtained at a brightness of 100 cd/m². ^c Obtained at a brightness of 1000 cd/m².

device showed higher maximum brightness with maximum luminance of 13287 cd/m² compared with 10968 cd/m² of PVK device. Lower operation voltage and higher luminance make our device more efficient, which was witnessed in the luminance efficiency curves as depicted in Figure 5. Our device exhibited higher luminance efficiency than PVK device in the whole measuring voltages range from 0 to 21 V. The maximum luminance efficiencies were 14.2 and 13.3 cd/A for PVPFK and PVK device, respectively, and the maximum power efficiencies were 2.8 and 2.4 lm/W for PVPFK and PVK device, respectively (for details, see Table 1). Another thing worth mentioning is that the maximum efficiency of our device was obtained in the practical luminance range of 100–1000 cd/m², which means more useful for commercial application.

As for the EL spectra of the blue PPLEDs, only blue emission was observed with peak at 476 nm and a shoulder at around 500 nm, and no high-energy shortwave emission from PVPFK or PVK host was observed, suggesting efficient energy from the host to the dopant phosphor emitter (for details, see Figure 6). Similar emission spectra from both PVPFK and PVK devices indicate the same mechanism involved in the EL process. But our device showed a little bluer emission compared with the PVK device, which was mirrored in the weaker shoulder and smaller full width at half-maximum (fwhm). The fwhm was 60.9 nm for the PVPFK device while the PVK device was 65.5 nm. And thus the corresponding Commission of International de l'Eclairage (CIE) coordinates x , y were (0.152, 0.379) and (0.161, 0.398) for the PVPFK and PVK devices, respectively. Blue emission spectrum of the blue PPLEDs indicates that PVPFK was more suitable than PVK as a blue phosphorescent host material.

CONCLUSIONS

We have proposed a strategy of steric hindrance functionalization of π -stacked polymers to control their electronic structures and phase behaviors. A solution-processable π -stacked homopolymer host with a congested conformation, PVPFK, has been successfully designed and synthesized through the typical vinyl polymerization of vinylcarbazole monomers containing cardo-type bulky frameworks. Photophysical and electrochemical studies show that PVPFK has the E_T level of 2.80 eV with the better electron-transporting ability than PVK. Proof-of-concept PPLEDs have been fabricated using PVPFK as host and Irpic as blue guest. The comparative study on PVPFK device and PVK device shows that this hindrance-functionalized π -stacked polymer, PVPFK, is a more effective host material for blue PPLEDs than PVK. The PVPFK-based device exhibited the lower operation voltage, higher luminance efficiency, and better CIE coordinate and EL efficiency than the PVK device under the same conditions.

ASSOCIATED CONTENT

S Supporting Information. Structural characterizations and phosphorescence spectra for the new compounds. This

material is available free of charge via the Internet at <http://pubs.acs.org>.

AUTHOR INFORMATION

Corresponding Author

*E-mail: iamlxie@njupt.edu.cn (L.-H.X.); wei-huang@njupt.edu.cn (W.H.).

ACKNOWLEDGMENT

The project was supported by the National Key Basic Research Program of China (973) (2009CB930600), National Natural Science Foundation of China (60876010, 20704023, 20974046, 21003076), Key Project of the Ministry of Education of China (104246, 208050), and Natural Science Foundation of Jiangsu Province (BK2008053, 200805005, 200907003, 10KJB510013, 09KJB150009, SJ209003).

REFERENCES

- (1) Lamansky, S.; Djurovich, P.; Murphy, D.; Abdel-Razzaq, F.; Lee, H.; Adachi, C.; Burrows, P.; Forrest, S.; Thompson, M. *J. Am. Chem. Soc.* **2001**, *123*, 4304–4312.
- (2) Adachi, C.; Baldo, M.; Thompson, M.; Forrest, S. *J. Appl. Phys.* **2001**, *90*, 5048–5051.
- (3) Sun, Y.; Giebink, N.; Kanno, H.; Ma, B.; Thompson, M.; Forrest, S. *Nature* **2006**, *440*, 908–912.
- (4) Kawamura, Y.; Goushi, K.; Brooks, J.; Brown, J.; Sasabe, H.; Adachi, C. *Appl. Phys. Lett.* **2005**, *86*, 071104–071106.
- (5) Ye, S.; Liu, Y.; Di, C.; Xi, H.; Wu, W.; Wen, Y.; Lu, K.; Du, C.; Yu, G. *Chem. Mater.* **2009**, *21*, 1333–1342.
- (6) Shih, P. I.; Chien, C. H.; Wu, F. I.; Shu, C. F. *Adv. Funct. Mater.* **2007**, *17*, 3514–3520.
- (7) Fan, C.; Chen, Y.; Gan, P.; Yang, C.; Zhong, C.; Qin, J.; Ma, D. *Org. Lett.* **2010**, *12*, 5648–5651.
- (8) Shih, P. I.; Chiang, C. L.; Dixit, A. K.; Chen, C. K.; Yuan, M. C.; Lee, R. Y.; Chen, C. T.; Diau, E. W. G.; Shu, C. F. *Org. Lett.* **2006**, *8*, 2799–2802.
- (9) Gong, X.; Robinson, M.; Ostrowski, J.; Moses, D.; Bazan, G.; Heeger, A. *Adv. Mater.* **2002**, *14*, 581–585.
- (10) Tokito, S.; Iijima, T.; Suzuri, Y.; Kita, H.; Tsuzuki, T.; Sato, F. *Appl. Phys. Lett.* **2003**, *83* (569), 569–511.
- (11) Holmes, R.; Forrest, S.; Tung, Y. J.; Kwong, R.; Brown, J.; Garon, S. *Appl. Phys. Lett.* **2003**, *82*, 2422–2424.
- (12) Adachi, C.; Kwong, R. C.; Djurovich, P.; Adamovich, V.; Baldo, M. A.; Thompson, M. E.; Forrest, S. R. *Appl. Phys. Lett.* **2001**, *79*, 2082–2084.
- (13) Sudhakar, M.; Djurovich, P.; Hogen-Esch, T.; Thompson, M. *J. Am. Chem. Soc.* **2003**, *125*, 7796–7797.
- (14) Chen, F.; Chang, S.; He, G.; Pyo, S.; Yang, Y.; Kurotaki, M.; Kido, J. *J. Polym. Sci., Part B: Polym. Phys.* **2003**, *41*, 2681–2690.
- (15) Chen, F.; He, G.; Yang, Y. *Appl. Phys. Lett.* **2003**, *82*, 1006–1008.
- (16) Monkman, A.; Burrows, H.; Hartwell, L.; Horsburgh, L.; Hamblett, I.; Navaratnam, S. *Phys. Rev. Lett.* **2001**, *86*, 1358–1361.
- (17) A. van Dijken, A.; Bastiaansen, J. J. A. M.; Kikken, N. M. M.; Langeveld, B. M. W. *J. Am. Chem. Soc.* **2004**, *126*, 7718–7727.

- (18) Chen, Y.; Huang, G.; Hsiao, C.; Chen, S. *J. Am. Chem. Soc.* **2006**, *128*, 8549–8558.
- (19) Wu, Z.; Xiong, Y.; Zou, J.; Wang, L.; Liu, J.; Chen, Q.; Yang, W.; Peng, J. *Adv. Mater.* **2008**, *20*, 2359–2364.
- (20) Chan, K.; Watkins, S.; Mak, C.; McKiernan, M.; Towns, C.; Pascu, S.; Holmes, A. *Chem. Commun.* **2005**, 2005, 5766–5768.
- (21) Liu, J.; Pei, Q. *Macromolecules* **2010**, *43*, 9608–9612.
- (22) Yeh, H. C.; Chien, C. H.; Shih, P. L.; Yuan, M. C.; Shu, C. F. *Macromolecules* **2008**, *41*, 3801–3807.
- (23) Xie, L. H.; Ling, Q. D.; Hou, X. Y.; Huang, W. *J. Am. Chem. Soc.* **2008**, *130*, 2120–2121.
- (24) Xie, L. H.; Deng, X. Y.; Chen, L.; Chen, S. F.; Liu, R. R.; Hou, X. Y.; Wong, K. Y.; Ling, Q. D.; Huang, W. *J. Polym. Sci., Part A: Polym. Chem.* **2009**, *47*, 5221–5229.
- (25) Yang, X.; Müller, D.; Neher, D.; Meerholz, K. *Adv. Mater.* **2006**, *18*, 948–954.
- (26) Lee, C.; Lee, K.; Kim, J. *Appl. Phys. Lett.* **2000**, *77*, 2280–2282.
- (27) Gong, X.; Ostrowski, J.; Bazan, G.; Moses, D.; Heeger, A. *Appl. Phys. Lett.* **2002**, *81*, 3711–3713.
- (28) Ye, T.; Chen, J.; Ma, D. *Phys. Chem. Chem. Phys.* **2010**, *12*, 15410–15431.
- (29) Tanaka, I.; Tabata, Y.; Tokito, S. *Chem. Phys. Lett.* **2004**, *400*, 86–89.
- (30) Mathai, M. K.; Choong, V. E.; Choulis, S. A.; Krummacker, B.; So, F. *Appl. Phys. Lett.* **2006**, *88*, 243512–24514.
- (31) Lee, C. C.; Yeh, K. M.; Chen, Y. *Polymer* **2008**, *49*, 4211–4217.
- (32) Yeh, K. M.; Lee, C. C.; Chen, Y. *Synth. Met.* **2008**, *158*, 565–571.
- (33) Ma, B.; Kim, B. J.; Deng, L.; Poulsen, D. A.; Thompson, M. E. *Macromolecules* **2007**, *40*, 8156–8161.
- (34) Debeaux, M.; Thesen, M. W.; Schneidenbach, D.; Hopf, H.; Janietz, S. *Adv. Funct. Mater.* **2010**, *20*, 399–408.
- (35) Thesen, M. W.; Höfer, B.; Debeaux, M.; Janietz, S.; Wedel, A.; Köhler, A.; Johannes, H. H.; Krueger, H. *J. Polym. Sci., Part A: Polym. Chem.* **2010**, *48*, 3417–3430.
- (36) Lee, C. C.; Yeh, K. M.; Chen, Y. *Polymer* **2009**, *50*, 410–417.
- (37) Wu, C.; Liu, T.; Hung, W.; Lin, Y.; Wong, K.; Chen, R.; Chen, Y.; Chien, Y. *J. Am. Chem. Soc.* **2003**, *125*, 3710–3711.
- (38) Xie, L.; Hou, X.; Hua, Y.; Tang, C.; Liu, F.; Fan, Q.; Huang, W. *Org. Lett.* **2006**, *8*, 3701–3704.
- (39) Bogdal, D.; Jaskot, K. *Synth. Commun.* **2000**, *30*, 3341–3352.
- (40) Xie, L. H.; Hou, X. Y.; Hua, Y. R.; Tang, C.; Liu, F.; Fan, Q. L.; Huang, W. *Org. Lett.* **2006**, *8*, 3701–3704.
- (41) Pascal de Sainte Claire, P. *J. Phys. Chem. B* **2006**, *110*, 7334–7343.
- (42) Zhang, C.; Von Seggern, H.; Pakbaz, K.; Kraabel, B.; Schmidt, H.; Heeger, A. *Synth. Met.* **1994**, *62*, 35–40.
- (43) Yeh, H.; Chien, C.; Shih, P.; Yuan, M.; Shu, C. *Macromolecules* **2008**, *41*, 3801–3807.
- (44) Lee, D. H.; Xun, Z.; Chae, H.; Cho, S. *Synth. Met.* **2009**, *159*, 1640–1643.